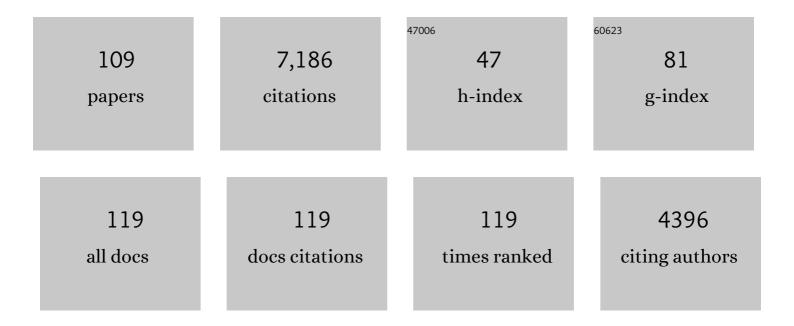
yann Klinger

List of Publications by Year in descending order

Source: https://exaly.com/author-pdf/8195738/publications.pdf Version: 2024-02-01



#	Article	IF	CITATIONS
1	Coseismic reverse- and oblique-slip surface faulting generated by the 2008 Mw 7.9 Wenchuan earthquake, China. Geology, 2009, 37, 515-518.	4.4	700
2	Primary surface ruptures of the great Himalayan earthquakes in 1934 and 1255. Nature Geoscience, 2013, 6, 71-76.	12.9	288
3	Roughness of fault surfaces over nine decades of length scales. Journal of Geophysical Research, 2012, 117, .	3.3	251
4	High-Resolution Satellite Imagery Mapping of the Surface Rupture and Slip Distribution of the Mw Â7.8, 14 November 2001 Kokoxili Earthquake, Kunlun Fault, Northern Tibet, China. Bulletin of the Seismological Society of America, 2005, 95, 1970-1987.	2.3	200
5	Estimating the return times of great Himalayan earthquakes in eastern Nepal: Evidence from the Patu and Bardibas strands of the Main Frontal Thrust. Journal of Geophysical Research: Solid Earth, 2014, 119, 7123-7163.	3.4	182
6	Characteristic slip for five great earthquakes along the Fuyun fault in China. Nature Geoscience, 2011, 4, 389-392.	12.9	170
7	Rupture process of the <i>M_w</i> = 7.9 2015 Gorkha earthquake (Nepal): Insights into Himalayan megathrust segmentation. Geophysical Research Letters, 2015, 42, 8373-8382.	4.0	170
8	Slip rate on the Dead Sea transform fault in northern Araba valley (Jordan). Geophysical Journal International, 2000, 142, 755-768.	2.4	158
9	Fault slip and earthquake recurrence along strike-slip faults — Contributions of high-resolution geomorphic data. Tectonophysics, 2015, 638, 43-62.	2.2	156
10	Structural Setting of the 2008 Mw 7.9 Wenchuan, China, Earthquake. Bulletin of the Seismological Society of America, 2010, 100, 2713-2735.	2.3	155
11	Lateral Offsets on Surveyed Cultural Features Resulting from the 1999 Izmit and Duzce Earthquakes, Turkey. Bulletin of the Seismological Society of America, 2002, 92, 79-94.	2.3	148
12	Coseismic deformation of the 2001Mw= 7.8 Kokoxili earthquake in Tibet, measured by synthetic aperture radar interferometry. Journal of Geophysical Research, 2005, 110, .	3.3	143
13	Relation between continental strikeâ€slip earthquake segmentation and thickness of the crust. Journal of Geophysical Research, 2010, 115, .	3.3	132
14	September 2005 Manda Hararoâ€Đabbahu rifting event, Afar (Ethiopia): Constraints provided by geodetic data. Journal of Geophysical Research, 2009, 114, .	3.3	129
15	Slip rate on the Kunlun fault at Hongshui Gou, and recurrence time of great events comparable to the 14/11/2001, Mwâ^¼7.9 Kokoxili earthquake. Earth and Planetary Science Letters, 2005, 237, 285-299.	4.4	128
16	Surface ruptures following the 30 October 2016 <i>M</i> _w 6.5 Norcia earthquake, central Italy. Journal of Maps, 2018, 14, 151-160.	2.0	121
17	Seismic behaviour of the Dead Sea fault along Araba valley, Jordan. Geophysical Journal International, 2000, 142, 769-782.	2.4	120
18	Evidence for an earthquake barrier model from Mwâ^¼7.8 Kokoxili (Tibet) earthquake slip-distribution. Earth and Planetary Science Letters, 2006, 242, 354-364.	4.4	120

#	Article	IF	CITATIONS
19	Measurement of ground displacement from optical satellite image correlation using the free open-source software MicMac. ISPRS Journal of Photogrammetry and Remote Sensing, 2015, 100, 48-59.	11.1	114
20	Slip rate and locking depth from GPS profiles across the southern Dead Sea Transform. Journal of Geophysical Research, 2008, 113, .	3.3	109
21	Active thrusting offshore Mount Lebanon: Source of the tsunamigenic A.D. 551 Beirut-Tripoli earthquake. Geology, 2007, 35, 755.	4.4	108
22	Active faulting in the Gulf of Aqaba: New knowledge from the <i>M</i> W 7.3 earthquake of 22 November 1995. Bulletin of the Seismological Society of America, 1999, 89, 1025-1036.	2.3	99
23	Co-Registration of Optically Sensed Images and Correlation (COSI-Corr): an operational methodology for ground deformation measurements. , 2007, , .		94
24	Millennial Recurrence of Large Earthquakes on the Haiyuan Fault near Songshan, Gansu Province, China. Bulletin of the Seismological Society of America, 2007, 97, 14-34.	2.3	94
25	Dynamics, Radiation, and Overall Energy Budget of Earthquake Rupture With Coseismic Offâ€Fault Damage. Journal of Geophysical Research: Solid Earth, 2019, 124, 11771-11801.	3.4	93
26	Serial ruptures of the San Andreas fault, Carrizo Plain, California, revealed by three-dimensional excavations. Journal of Geophysical Research, 2006, 111, n/a-n/a.	3.3	92
27	Slip deficit in central Nepal: omen for a repeat of the 1344 AD earthquake?. Earth, Planets and Space, 2016, 68, .	2.5	89
28	A database of the coseismic effects following the 30 October 2016 Norcia earthquake in Central Italy. Scientific Data, 2018, 5, 180049.	5.3	89
29	12,000-Year-Long Record of 10 to 13 Paleoearthquakes on the Yammouneh Fault, Levant Fault System, Lebanon. Bulletin of the Seismological Society of America, 2007, 97, 749-771.	2.3	88
30	Off-fault damage patterns due to supershear ruptures with application to the 2001Mw8.1 Kokoxili (Kunlun) Tibet earthquake. Journal of Geophysical Research, 2007, 112, .	3.3	82
31	Long-term slip rate of the southern San Andreas Fault from10Be-26Al surface exposure dating of an offset alluvial fan. Journal of Geophysical Research, 2006, 111, .	3.3	77
32	Earthquake Damage Patterns Resolve Complex Rupture Processes. Geophysical Research Letters, 2018, 45, 10,279.	4.0	74
33	Fault-Scarp Features and Cascading-Rupture Model for the Mw 7.9 Wenchuan Earthquake, Eastern Tibetan Plateau, China. Bulletin of the Seismological Society of America, 2010, 100, 2590-2614.	2.3	73
34	Surface Rupture and Slip Distribution of the 1940 Imperial Valley Earthquake, Imperial Fault, Southern California: Implications for Rupture Segmentation and Dynamics. Bulletin of the Seismological Society of America, 2013, 103, 629-640.	2.3	73
35	Sources of the large A.D. 1202 and 1759 Near East earthquakes. Geology, 2005, 33, 529.	4.4	69
36	Reevaluation of surface rupture parameters and faulting segmentation of the 2001 Kunlunshan earthquake (Mw7.8), northern Tibetan Plateau, China. Journal of Geophysical Research, 2006, 111, n/a-n/a.	3.3	69

#	Article	IF	CITATIONS
37	Slip-Partitioned Surface Breaks for the Mw 7.8 2001 Kokoxili Earthquake, China. Bulletin of the Seismological Society of America, 2005, 95, 731-738.	2.3	67
38	The 14 November 2001 Kokoxili (Tibet) earthquake: Highâ€frequency seismic radiation originating from the transitions between subâ€Rayleigh and supershear rupture velocity regimes. Journal of Geophysical Research, 2008, 113, .	3.3	67
39	Paleoseismic Evidence of Characteristic Slip on the Western Segment of the North Anatolian Fault, Turkey. Bulletin of the Seismological Society of America, 2003, 93, 2317-2332.	2.3	64
40	Inference of Multiple Earthquake-Cycle Relaxation Timescales from Irregular Geodetic Sampling of Interseismic Deformation. Bulletin of the Seismological Society of America, 2013, 103, 2824-2835.	2.3	64
41	Stress tensor and focal mechanisms along the Dead Sea fault and related structural elements based on seismological data. Tectonophysics, 2007, 429, 165-181.	2.2	63
42	The 14 November 2001, Mw = 7.8 Kokoxili Earthquake in Northern Tibet (Qinghai Province, China). Seismological Research Letters, 2002, 73, 125-135.	1.9	57
43	Subsidence and Sinkhole Hazard Assessment in the Southern Dead Sea Area, Jordan. Pure and Applied Geophysics, 2005, 162, 221-248.	1.9	56
44	Probing large intraplate earthquakes at the west flank of the Andes. Geology, 2014, 42, 1083-1086.	4.4	54
45	Geologic Inheritance and Earthquake Rupture Processes: The 1905 MÂ≥Â8 Tsetserlegâ€Bulnay Strikeâ€Slip Earthquake Sequence, Mongolia. Journal of Geophysical Research: Solid Earth, 2018, 123, 1925-1953.	3.4	53
46	Alluvial deposition and lake-level fluctuations forced by Late Quaternary climate change: the Dead Sea case example. Sedimentary Geology, 2003, 162, 119-139.	2.1	52
47	Variability in magnitude of paleoearthquakes revealed by trenching and historical records, along the Haiyuan Fault, China. Journal of Geophysical Research: Solid Earth, 2015, 120, 8304-8333.	3.4	51
48	Six similar sequential ruptures of the San Andreas fault, Carrizo Plain, California. Geology, 2004, 32, 649.	4.4	50
49	5000 yr of paleoseismicity along the southern Dead Sea fault. Geophysical Journal International, 2015, 202, 313-327.	2.4	49
50	Modes and rates of horizontal deformation from rotated river basins: Application to the Dead Sea fault system in Lebanon. Geology, 2015, 43, 843-846.	4.4	47
51	Measuring radon flux across active faults: Relevance of excavating and possibility of satellite discharges. Radiation Measurements, 2010, 45, 211-218.	1.4	46
52	Variable behavior of the Dead Sea Fault along the southern Arava segment from GPS measurements. Comptes Rendus - Geoscience, 2015, 347, 161-169.	1.2	46
53	The Burstâ€Like Behavior of Aseismic Slip on a Rough Fault: The Creeping Section of the Haiyuan Fault, China. Bulletin of the Seismological Society of America, 2015, 105, 480-488.	2.3	41
54	Slip deficit and temporal clustering along the Dead Sea fault from paleoseismological investigations. Scientific Reports, 2018, 8, 4511.	3.3	39

#	Article	IF	CITATIONS
55	Palaeoseismology of the North Anatolian Fault near the Marmara Sea: implications for fault segmentation and seismic hazard. Geological Society Special Publication, 2009, 316, 31-54.	1.3	38
56	Magma influence on propagation of normal faults: Evidence from cumulative slip profiles along Dabbahu-Manda-Hararo rift segment (Afar, Ethiopia). Journal of Structural Geology, 2017, 95, 48-59.	2.3	37
57	High-resolution mapping based on an Unmanned Aerial Vehicle (UAV) to capture paleoseismic offsets along the Altyn-Tagh fault, China. Scientific Reports, 2017, 7, 8281.	3.3	35
58	Reevaluation of the Late Pleistocene Slip Rate of the Haiyuan Fault Near Songshan, Gansu Province, China. Journal of Geophysical Research: Solid Earth, 2019, 124, 5217-5240.	3.4	35
59	Geological structures control on earthquake ruptures: The <i>M_w</i> 7.7, 2013, Balochistan earthquake, Pakistan. Geophysical Research Letters, 2016, 43, 10,155.	4.0	34
60	Early Holocene and Late Pleistocene slip rates of the southern Dead Sea Fault determined from ¹⁰ Be cosmogenic dating of offset alluvial deposits. Journal of Geophysical Research, 2010, 115, .	3.3	33
61	Quaternary morphotectonic mapping of the Wadi Araba and implications for the tectonic activity of the southern Dead Sea fault. Tectonics, 2012, 31, .	2.8	32
62	A Paleoseismic Record of Earthquakes for the Dead Sea Transform Fault between the First and Seventh Centuries C.E.: Nonperiodic Behavior of a Plate Boundary Fault. Bulletin of the Seismological Society of America, 2014, 104, 1329-1347.	2.3	32
63	Horizontal surface-slip distribution through several seismic cycles: The Eastern Bogd fault, Gobi-Altai, Mongolia. Tectonophysics, 2018, 734-735, 167-182.	2.2	32
64	The 2016 M7 Kumamoto, Japan, Earthquake Slip Field Derived From a Joint Inversion of Differential Lidar Topography, Optical Correlation, and InSAR Surface Displacements. Geophysical Research Letters, 2019, 46, 6341-6351.	4.0	30
65	Review of On-Fault Palaeoseismic Studies Along the Dead Sea Fault. Modern Approaches in Solid Earth Sciences, 2014, , 183-205.	0.3	30
66	Which Fault Segments Ruptured in the 2008 Wenchuan Earthquake and Which Did Not? New Evidence from Nearâ€Fault 3D Surface Displacements Derived from SAR Image Offsets. Bulletin of the Seismological Society of America, 2017, 107, 1185-1200.	2.3	29
67	Variable slip-rate and slip-per-event on a plate boundary fault: The Dead Sea fault in northern Israel. Tectonophysics, 2018, 722, 210-226.	2.2	27
68	Ejection Landslide at Northern Terminus of Beichuan Rupture Triggered by the 2008 Mw 7.9 Wenchuan Earthquake. Bulletin of the Seismological Society of America, 2010, 100, 2689-2699.	2.3	26
69	Localised and distributed deformation in the lithosphere: Modelling the Dead Sea region in 3 dimensions. Earth and Planetary Science Letters, 2011, 308, 172-184.	4.4	26
70	Seismotectonics of southern Haiti: A new faulting model for the 12 January 2010 <i>M</i> 7.0 earthquake. Geophysical Research Letters, 2015, 42, 10,273.	4.0	26
71	Influence of fault roughness on surface displacement: from numerical simulations to coseismic slip distributions. Geophysical Journal International, 2020, 220, 1857-1877.	2.4	26
72	The M w 7.9, 12 May 2008 Sichuan earthquake rupture measured by sub-pixel correlation of ALOS PALSAR amplitude images. Earth, Planets and Space, 2010, 62, 875-879.	2.5	25

#	Article	IF	CITATIONS
73	Active Faults' Geometry in the Gulf of Aqaba, Southern Dead Sea Fault, Illuminated by Multibeam Bathymetric Data. Tectonics, 2021, 40, e2020TC006443.	2.8	25
74	Earthquake crisis unveils the growth of an incipient continental fault system. Nature Communications, 2019, 10, 3482.	12.8	24
75	Recent progress in studies on the characteristics of surface rupture associated with large earthquakes. Journal of the Geological Society of Korea, 2017, 53, 129-157.	0.7	24
76	Co-seismic deformation during the Mw7.3 Aqaba Earthquake (1995) from ERS-SAR interferometry. Geophysical Research Letters, 2000, 27, 3651-3654.	4.0	22
77	Localized slip and distributed deformation in oblique settings: the example of the Denali fault system, Alaska. Geophysical Journal International, 2014, 197, 1284-1298.	2.4	22
78	Crustal accretion at a sedimented spreading center in the Andaman Sea. Geology, 2016, 44, 351-354.	4.4	22
79	Detailed map, displacement, paleoseismology, and segmentation of the Enriquillo-Plantain Garden Fault in Haiti. Tectonophysics, 2020, 778, 228368.	2.2	22
80	Post Earthquake Aggradation Processes to Hide Surface Ruptures in Thrust Systems: The M8.3, 1934, Biharâ€Nepal Earthquake Ruptures at Charnath Khola (Eastern Nepal). Journal of Geophysical Research: Solid Earth, 2019, 124, 9182-9207.	3.4	21
81	Complex Deformation at Shallow Depth During the 30 October 2016 M w 6.5 Norcia Earthquake: Interference Between Tectonic and Gravity Processes?. Tectonics, 2020, 39, e2019TC005596.	2.8	21
82	Introduction to the Special Issue on the 2008 Wenchuan, China, Earthquake. Bulletin of the Seismological Society of America, 2010, 100, 2353-2356.	2.3	20
83	Complex surface rupturing and related formation mechanisms in the Xiaoyudong area for the 2008 Mw 7.9 Wenchuan Earthquake, China. Journal of Asian Earth Sciences, 2012, 58, 132-142.	2.3	20
84	Inelastic surface deformation during the 2013 M _w 7.7 Balochistan, Pakistan, earthquake. Geology, 0, , G37290.1.	4.4	20
85	Lower Crustal Heterogeneity Beneath the Northern Tibetan Plateau Constrained by GPS Measurements Following the 2001 Mw7.8 Kokoxili Earthquake. Journal of Geophysical Research: Solid Earth, 2019, 124, 11992-12022.	3.4	20
86	Surface displacements on faults triggered by slow magma transfers between dyke injections in the 2005–2010 rifting episode at Dabbahu–Manda–Hararo rift (Afar, Ethiopia). Geophysical Journal International, 2016, 204, 399-417.	2.4	19
87	Late Pleistocene slip rate of the central Haiyuan fault constrained from optically stimulated luminescence, 14C, and cosmogenic isotope dating and high-resolution topography. Bulletin of the Geological Society of America, 2021, 133, 1347-1369.	3.3	18
88	Late Pleistoceneâ€Holocene Slip Rate Along the Hasi Shan Restraining Bend of the Haiyuan Fault: Implication for Faulting Dynamics of a Complex Fault System. Tectonics, 2019, 38, 4127-4154.	2.8	17
89	Experimental evidence for crustal control over seismic fault segmentation. Geology, 2020, 48, 844-848.	4.4	17
90	REFINED SATELLITE IMAGE ORIENTATION IN THE FREE OPEN-SOURCE PHOTOGRAMMETRIC TOOLS APERO/MICMAC. ISPRS Annals of the Photogrammetry, Remote Sensing and Spatial Information Sciences, 0, III-1, 83-90.	0.0	16

#	Article	IF	CITATIONS
91	Fault Segmentation Pattern Controlled by Thickness of Brittle Crust. Geophysical Research Letters, 2021, 48, e2021GL093390.	4.0	15
92	Fault Geometry and Slip Distribution of the 2013 Mw 7.7 Balochistan Earthquake From Inversions of SAR and Optical Data. Journal of Geophysical Research: Solid Earth, 2020, 125, e2019JB018380.	3.4	14
93	Rupture behavior and deformation localization of the Kunlunshan earthquake (M w 7.8) and their tectonic implications. Science in China Series D: Earth Sciences, 2008, 51, 1361-1374.	0.9	13
94	Seismotectonics of the 2008 and 2009 Qaidam Earthquakes and its Implication for Regional Tectonics. Acta Geologica Sinica, 2013, 87, 618-628.	1.4	12
95	REFINED SATELLITE IMAGE ORIENTATION IN THE FREE OPEN-SOURCE PHOTOGRAMMETRIC TOOLS APERO/MICMAC. ISPRS Annals of the Photogrammetry, Remote Sensing and Spatial Information Sciences, 0, III-1, 83-90.	0.0	11
96	Active tectonics along the Cul-de-Sac – Enriquillo plain and seismic hazard for Port-au-Prince, Haiti. Tectonophysics, 2019, 771, 228235.	2.2	9
97	Similarities between mode III crack growth patterns and strike-slip faults. Philosophical Transactions Series A, Mathematical, Physical, and Engineering Sciences, 2019, 377, 20170392.	3.4	9
98	Source Model of the 2014 MwÂ6.9 Yutian Earthquake at the Southwestern End of the Altyn Tagh Fault in Tibet Estimated from Satellite Images. Seismological Research Letters, 2020, 91, 3161-3170.	1.9	9
99	High-resolution stratigraphy and multiple luminescence dating techniques to reveal the paleoseismic history of the central Dead Sea fault (Yammouneh fault, Lebanon). Tectonophysics, 2018, 738-739, 1-15.	2.2	8
100	Assessing the brittle crust thickness from strike-slip fault segments on Earth, Mars and Icy moons. Tectonophysics, 2021, 805, 228779.	2.2	8
101	25,000 Years long seismic cycle in a slow deforming continental region of Mongolia. Scientific Reports, 2021, 11, 17855.	3.3	8
102	Rifting Processes at a Continentâ€Ocean Transition Rift Revealed by Fault Analysis: Example of Dabbahuâ€Mandaâ€Hararo Rift (Ethiopia). Tectonics, 2019, 38, 190-214.	2.8	6
103	Imaging normal faults in alluvial fans using geophysical techniques: Field example from the coast of Gulf of Aqaba, Saudi Arabia. , 2014, , .		6
104	Signature of transition to supershear rupture speed in the coseismic off-fault damage zone. Proceedings of the Royal Society A: Mathematical, Physical and Engineering Sciences, 2021, 477, 20210364.	2.1	6
105	Late Quaternary Slip Rate of the Zihong Shan Branch and Its Implications for Strain Partitioning Along the Haiyuan Fault, Northeastern Tibetan Plateau. Journal of Geophysical Research: Solid Earth, 2022, 127, .	3.4	5
106	Interseismic deformation in the Gulf of Aqaba from GPS measurements. Geophysical Journal International, 2021, 228, 477-492.	2.4	3
107	Segmentation and Holocene Behavior of the Middle Strand of the North Anatolian Fault (NW Turkey). Tectonics, 2021, 40, e2021TC006870.	2.8	3
108	Imprint of the Continental Strikeâ€ S lip Fault Geometrical Structure in Geophysical Data. Geophysical Research Letters, 2022, 49	4.0	3

#	Article	IF	CITATIONS
109	Sismotectonique du tremblement de terre du 12 janvier 2010 en HaÃ ⁻ ti. Outre-Terre, 2013, nº 35-36, 163-183.	0.0	1